Reaustenisation Kinetics of Martensite – Technical Notes

The reaustenisation of a martensitic structure has been implemented in JMatPro-V12 as an additional feature to the existing structure types of either normalised (coarse) or quenched-tempered (fine). We now have reaustenitisation models for all possible phases, including ferrite, pearlite, bainite and martensite.

The model utilises a modified Johnson-Mehl-Avrami equation that is similar to the one used in the reaustenitisation of normalised or quenched-tempered structure, but there are also noticeable differences. In the case of the normalised or quenched-tempered structure, the starting microstructure is considered to be a mixture of ferrite and pearlite/carbides. The transformation occurs by pearlite transforming to austenite first, followed by the transformation of the austenite+ferrite mixture to austenite, and the reaustenisation kinetics are limited by C diffusion. In the case of the martensitic structure, the assumption is that martensite transforms to austenite directly without involving any intermediate stages. The kinetics of martensite reaustenisation can be controlled by either C diffusion or M diffusion, where M stands for substitutional elements, because martensite can form in steels with or without carbon.

A calculated TTA diagram for steel 3310 of martensitic structure is shown in Fig. 1 as an example. The kinetics is controlled by C diffusion in this alloy. A typical TTA diagram contains three curves, labelled as Ac_1, Ac_3 and Homog. Aust. The Ac_1 and Ac_3 curves correspond to the start and completion of reaustenitisation, respectively. The initial structure of the transformed austenite will be inhomogeneous, in that concentration profiles for the non-interstitial elements in the starting microstructure remains. This transformed austenite will "homogenise" as a function of time and temperature after reaustenisation is complete, and the Homog. Aust. curve denotes the completion of this homogenisation process.

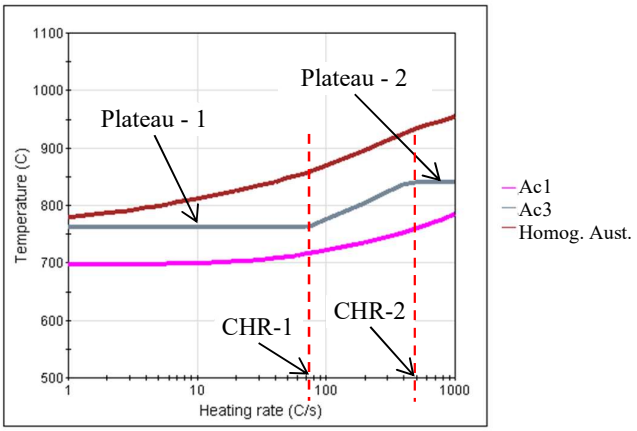

Fig. 1: TTA diagrams of steel 3310 of martensitic structure.

The A_{3r} curve contains two plateaus as can be seen in Fig. 1, characterised by two critical heating rates CHR-1 and CHR-2. There are two constrains in the reaustenitisation process: one is the transformation kinetics controlled by diffusion; the other is the maximum austenite amount limited by thermodynamic equilibrium. When heating at rates slower than CHR1, the transformation closely follows equilibrium, i.e. reaustenitisation completes whenever the equilibrium A_3 temperature is reached, resulting in Plateau-1. As the heating rate increases between CHR-1 and CHR-2, the temperature range between Ac_1 and Ac_3 begins to broaden and reaustenitisation completes at a temperature above the equilibrium A_3. On further increase of the heating rate above CHR-2, a quite different transformation may occur. This is because martensite or ferrite can transform to austenite in a massive, diffusionless way. In this case the Ac_3 temperature is essentially constant as function of cooling rate.

It is instructive to show the microstructure evolution during heating at various rates to better understand the plateaus in Fig. 1. Fig. 2 contains the reaustenitisation of alloy 3310 during heating at 10, 100, 500 and

1000°C/s. At 10°C/s, Fig. 2(a), martensite starts to transform to austenite at around 690°C via a diffusion-controlled process. When temperature reaches around 710°C, a reflection in the curve is observed. This is because austenite has reached its equilibrium amount at this temperature and cannot go beyond. Above this temperature, the austenite evolution follows the austenite approach curve until reaching Plateau-1, which is the equilibrium A_3 temperature. The austenite evolution during heating at 100°C/s starts at around 720°C and reaches completion at around 780°C, which is beyond A_3. At 500°C/s, Fig. 2(b), the early part of reaustenitisation is diffusion-controlled. However, when temperature reaches 840°C, martensite transforms to austenite in a diffusionless way, i.e. the so-called massive transformation. The austenite evolution at 1000°C/s also ends via this diffusionless mechanism at 840°C – shown as Plateau-2 in Fig. 1(a), though at a much slower pace at early stages, Fig. 2(b).

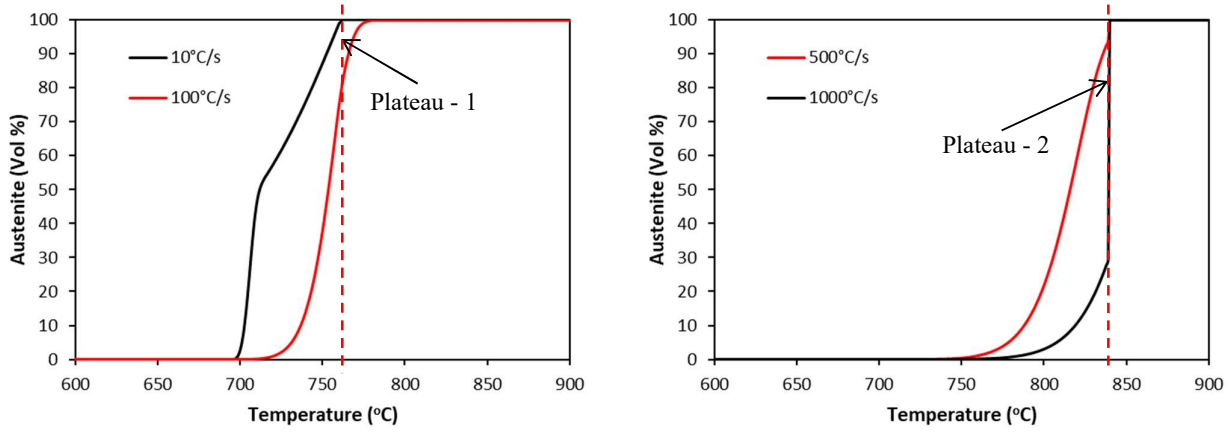

(a) (b)

Fig. 2: Austenite evolution in steel 3310 during heating at various rates: (a) 10 and 100°C/s, and (b) 500 and 1000°C/s.

Martensite can form in steels without little carbon, such as maraging steels, in which case the reaustenitisation would be controlled by the diffusion of substitutional elements, or M-controlled. The calculated TTA diagrams of maraging steels PH13-8Mo and C300 are shown in Fig. 3 as examples, with experimental data taken from Refs. 1 and 2, respectively. Because the reaustenitisation kinetics is M-controlled, the "Homog. Aust." curve becomes irrelevant and has been removed.

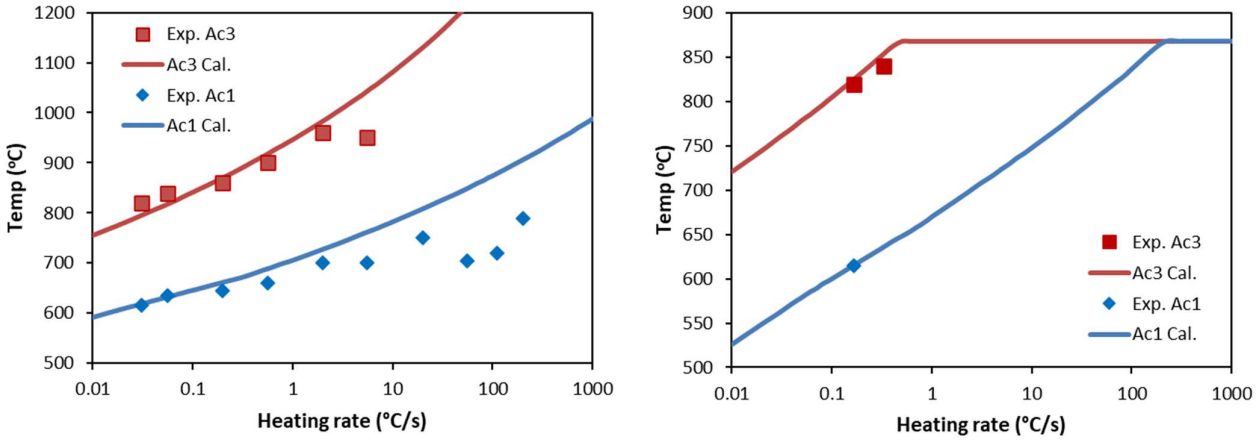

(a) PH13-8Mo (b) C300

Fig. 3: TTA diagrams of two maraging steels, (a) PH13-8Mo with experimental data from Ref. 1, and (b) C300 with experimental data from Ref. 2.

A common issue in the model development for reaustenitisation of a martensitic structure has been the lack of experimental data for model assessment. When the diffusion is M-controlled, e.g. maraging steels, there are experimental studies on the austenite reversion kinetics during aging, which form the basis of the current

model assessment. Fig. 4 shows the microstructural evolution in steel PH13-8Mo during aging at 575°C, with experimental data taken from Refs. 3 and 4, and grade 350 during aging at 640°C, with experimental data from Ref. 5.

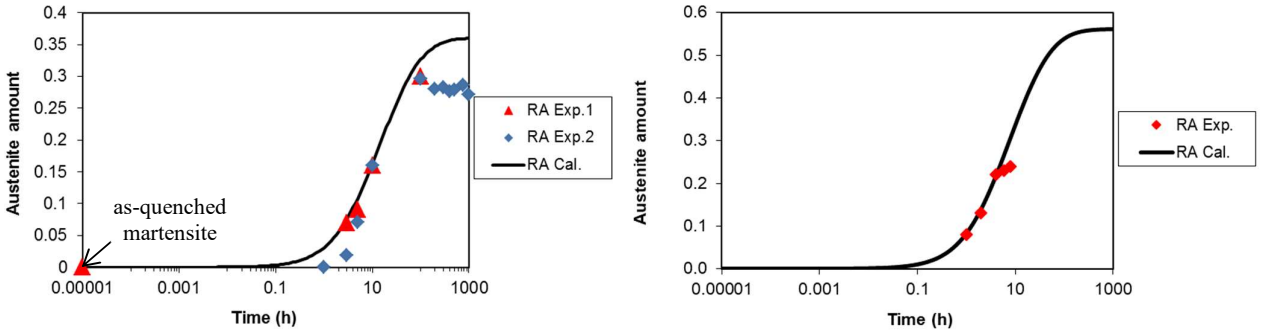

(a) PH13-8Mo (b) C350

Fig. 4: Austenite reversion during ageing of steel (a) PH13-8Mo at 575°C, and (b) C350 at 640°C. Experimental data in (a) were taken from Refs. 3 and 4, and (b), Ref. 5, respectively.

Experimental TTA diagrams were reported for two steels containing carbon of martensitic structure: one is steel 50CrMo4 of composition Fe-0.51C-0.32Si-0.68Mn-1.06Cr-0.14Cu-0.21Mn-0.014N-0.01Nb-0.15Ni-0.014V from Ref. 6. and the other is steel 10Kh3G3MF of composition Fe-0.1C-0.34Si-2.81Mn-2.77Cr-0.12V-0.4Mo from Ref. 7. Fig. 5 are the comparison plots between the calculated and experimental TTA diagrams for these two steels.

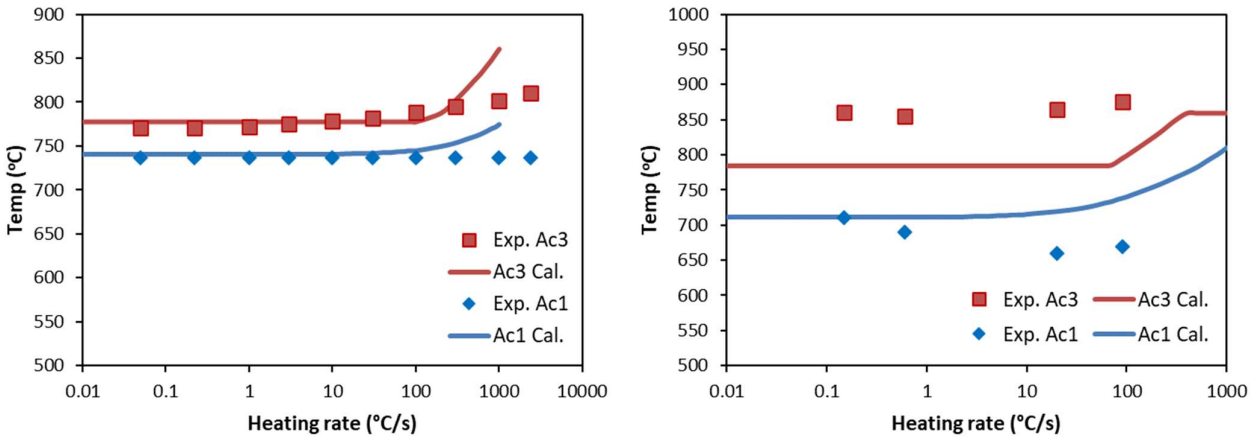

(a) 50CrMo4 (b) 10Kh3G3MF

Fig. 5: TTA diagrams of two steels containing carbon, (a) 50CrMo4 with experimental data from Ref. 6, and (b) 10Kh3G3MF with experimental data from Ref.7.

All steels, even maraging steels, contain traces of carbon, and consequently carbides in the microstructure. The following procedures are observed when determining whether C- or M-diffusion is on control.

- Find the maximum amount of carbides: M_3C, $M_2(C,N)$, M(C,N) and MN.
- Find the maximum amount of intermetallic phases: (FE,NI)AL, DELTA, ETA and CU.
- If the maximum amount of carbides is bigger, the reaustenitisation is considered to be controlled by C-diffusion, otherwise, by M-diffusion.

The real reaustenitisation process is rather complex. There is usually no clear indication of whether C-diffusion or M-diffusion is in control, and the austenite completion curve should fall in between the calculated curves of C-diffusion and M-diffusion, as shown in Fig. 6. The two TTA diagrams are for steels Fe-13Cr-6Ni-2Mo and Fe-3Si-13Cr-7Ni, with experimental data taken from Refs. 8 and 9, respectively. It

should be noted that Fe-13Cr-6Ni-2Mo is judged to be C-control, whereas Fe-3Si-13Cr-7Ni, M-control, in accordance with the above procedures.

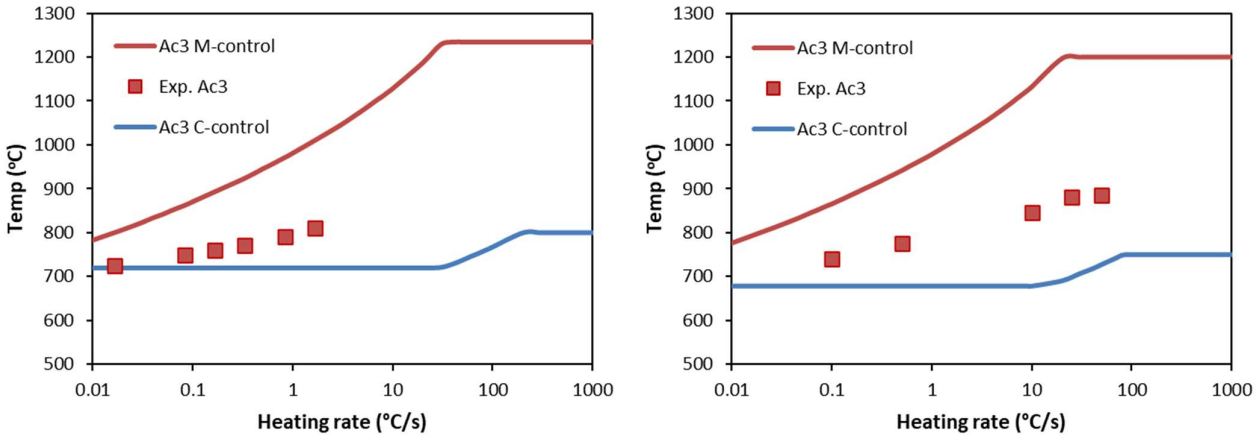

(a) Fe-13Cr-6Ni-2Mo (b) Fe-3Si-13Cr-7Ni

Fig. 6: TTA diagrams of two martensitic stainless steels, (a) Fe-13Cr-6Ni-2Mo with experimental data from Ref.8, and (b) Fe-3Si-13Cr-7Ni with experimental data from Ref. 9.

In summary, the reaustenitisation of a martensitic structure is a rather complex process. It is modelled as a one-stage transformation here but can contain more than one stage in reality [2,7]. The Ac_3 curve in a typical TTA diagram may contain two plateaus, representing the equilibrium A_3 temperature and the massive transformation temperature T_m, respectively. Both temperatures are calculated thermodynamically in the model, and their values are affected by the matrix composition used to carry out the calculation. The real matrix composition changes in a dynamic fashion, which adds to the complexity in determining the values of A_3 and T_m. On the other hand, the controlling mechanism can be either C-diffusion or M-diffusion in the model but the real process is probably somewhere in between.

References:

1. http://www.barc.gov.in/publications/eb/golden/material/toc/chapter9/9_2.pdf, accessed March 2020, Study of the martensite to austenite transformation in steels by dilatometry, in: Materials Science and Engineering, Bhabha Atomic Research Centre Publications.
2. A.G. Reis, D.A.P. Reis, A.J. Abdalla, J. Otubo and H.R.Z. Sandim, A dilatometric study of the continuous heating transformations in maraging 300 steel, IOP Conf. Series: Materials Science and Engineering 97 (2015), 012006.
3. R. Schnitzer, S. Zinner and H. Leitner, Modeling of the yield strength of a stainless maraging steel, Scripta Materialia 62 (2010), 286-289.
4. M. Schober, R. Schnitzer and H. Leitner, Precipitation evolution in a Ti-free and Ti-containing stainless maraging steel, Ultramicroscopy 109 (2009), 553-562.
5. U.K. Viswanathan, G.K. Dey and M.K. Asundi, Precipitation hardening in 350 grade maraging steel, Metall. Trans. A, 24A (1993), 2429-2442.
6. StahlDat SX, Atlas zur Wärmebehandlung der Stähle. Band 3: Zeit – Temperatur – Austenitisierung – Schaubilder. Von J. Orlich, A. Rose, P. Wieast. 1. Auflage, Verlag Stahleisen mbH, Düsseldorf. 1973.
7. D.O. Panov and A.I. Smirnov, Features of austenite formation in low-carbon steel upon heating in the intercritical temperature range, Physics of Metals and Metallography, 118 (2017), 1081–1090.
8. A. Bojack, L. Zhao, P.F. Morris and J. Sietsma, Austenite formation from aartensite in a 13Cr6Ni2Mo supermartensitic stainless steel, Metall. Mater. Trans. A, 47A (2016) 1996-2009.
9. Y.K. Lee, H.C. Shin, D.S. Leem, J.Y. Choi, W. Jin and C.S. Choi, Reverse transformation mechanism of martensite to austenite and amount of retained austenite after reverse transformation in Fe-3Si-13Cr-7Ni (wt%) martensitic stainless steel, Materials Science and Technology, 19 (2003) 393-398.